HHS Public Access

Author manuscript

Crit Care Med. Author manuscript; available in PMC 2020 March 01.

Published in final edited form as:

Crit Care Med. 2019 March ; 47(3): 410–418. doi:10.1097/CCM.0000000000003555.

Ferroptosis contributes to neuronal death and functional outcome after traumatic brain injury.

Elizabeth M. Kenny, BS[1,2,3], **Emin Fidan, MD**[1,2,3], **Qin Yang, MD**[1,2,3], **Tamil S. Anthonymuthu, PhD**[1,2,3], **Lee Ann New, BS**[1,2], **Elizabeth A. Meyer, BS**[1,2], **Hong Wang, PhD**[4], **Patrick M. Kochanek, MD**[2], **C. Edward Dixon, PhD**[2,5], **Valerian E. Kagan, PhD, DSc**[3,6], and **Hülya Bayır, MD**[1,2,3,6,7]

[1]Department of Critical Care Medicine, School of Medicine, University of Pittsburgh, Pittsburgh, PA, 15213

[2]Safar Center for Resuscitation Research, University of Pittsburgh, Pittsburgh, PA, 15213

[3]Center for Free Radical and Antioxidant Health, University of Pittsburgh, Pittsburgh, PA, 15213

[4]Department of Biostatistics, Graduate School of Public Health, University of Pittsburgh, Pittsburgh, PA, 15213

[5]Department of Neurosurgery, School of Medicine, University of Pittsburgh, Pittsburgh, PA, 15213

[6]Department of Environmental and Occupational Health, Graduate School of Public Health, University of Pittsburgh, Pittsburgh, PA, 15213

[7]Children's Hospital of Pittsburgh of UPMC, University of Pittsburgh, Pittsburgh, PA, 15213

Abstract

OBJECTIVES: Traumatic brain injury (TBI) triggers multiple cell death pathways, possibly including ferroptosis – a recently described cell death pathway that results from accumulation of 15-lipoxygenase (15-LOX)-mediated lipid oxidation products, specifically oxidized phosphatidylethanolamine (PE) containing arachidonic (AA) or adrenic (AdA) acid. This study aimed to investigate whether ferroptosis contributed to the pathogenesis of *in vitro* and *in vivo* TBI, and whether inhibition of 15-LOX provided neuroprotection.

DESIGN: Cell culture study and randomized, controlled animal study.

SETTING: University research laboratory.

SUBJECTS: HT22 neuronal cell line and adult male C57BL/6 mice.

Corresponding author: Hülya Bayır, MD, Professor, Department of Critical Care Medicine, Department of Environmental and Occupational Health, Director of Research, Pediatric Critical Care Medicine, Associate Director, Center for Free Radical and Antioxidant Health, Safar Center for Resuscitation Research, University of Pittsburgh, Phone: 412-383-7865. bayihx@ccm.upmc.edu.

No financial disclosures

Copyright form disclosure: Drs. Yang, Mayer, Kochanek, Dixon, Kagan, and Bayir received support for article research from the National Institutes of Health (NIH). Dr. Kochanek's institution received funding from the NIH; he received funding from Society of Critical Care Medicine (Editor-in-Chief of *Pediatric Critical Care Medicine*) and from serving as an expert witness and a visiting professor/grand rounds speaker (travel/compensation); and he disclosed other funding separate from that reported in this study by both the NIH, the US Department of Defense, and the state of Pennsylvania. Dr. Kagan disclosed government work. The remaining authors have disclosed that they do not have any potential conflicts of interest.

INTERVENTIONS: HT22 cells were subjected to pharmacologic induction of ferroptosis or mechanical stretch injury with and without administration of inhibitors of ferroptosis. Mice were subjected to sham or controlled cortical impact (CCI) injury. Injured mice were randomized to receive vehicle or baicalein (12/15-LOX inhibitor) at 10–15 min post-injury.

MEASUREMENTS AND MAIN RESULTS: Pharmacological inducers of ferroptosis and mechanical stretch injury resulted in cell death that was rescued by prototypical anti-ferroptotic agents including baicalein. Liquid chromatography tandem-mass spectrometry (LC-MS/MS) revealed the abundance of AA/AdA-PE compared to other AA/AdA-containing phospholipids in the brain. CCI resulted in accumulation of oxidized PE, increased expression of 15-LOX and acyl-CoA synthetase long-chain family member 4 (ACSL4; enzyme which generates substrate for the esterification of AA/AdA into PE), and depletion of glutathione in the ipsilateral cortex. Post-injury administration of baicalein attenuated oxidation of AA/AdA-PE, decreased the number of TUNEL positive cells in the hippocampus, and improved spatial memory acquisition vs vehicle.

CONCLUSIONS: Biomarkers of ferroptotic death were increased after TBI. Baicalein decreased ferroptotic PE oxidation and improved outcome after CCI, suggesting that 15-LOX pathway might be a valuable therapeutic target after TBI.

Keywords

Ferroptosis; Traumatic brain injury; Cell death; Lipoxygenase; Lipid oxidation; Baicalein

Introduction

Traumatic brain injury (TBI) is a critical health concern that results in significant morbidity, mortality, and financial cost worldwide (1–3). In the US alone, TBI accounts for approximately 2.5 million emergency department visits, 280,000 hospitalizations, and 52,000 deaths annually (1). Direct and indirect costs of TBI in the US approach $76.5 billion per year, with severe TBI accounting for 90% of this medical spending (4, 5). Despite the high burden of severe TBI, effective neuroprotective therapies are lacking with no clear improvement in overall outcome in more than two decades (6).

Neuronal death contributes to neurological deficit after TBI, and thus is a reasonable therapeutic target. Ferroptosis is a recently described, regulated cell death pathway that results from accumulation of lipid oxidation products (Fig. S1A) (7, 8). We recently showed that 15-lipoxygenase (LOX)-mediated oxidation of phosphatidylethanolamines (PE), specifically those containing arachidonic (AA) and adrenic acid (AdA), is a key step in ferroptosis execution (9, 10). Complex formation between 15-LOX and PE binding protein 1 (PEBP1) results in a change in 15-LOX substrate specificity from free to esterified AA (10). Acyl-CoA synthetase long-chain family member 4 (ACSL4) contributes to ferroptosis by generating substrate for the esterification of AA/AdA into PE (11). Glutathione peroxidase 4 (GPX4) is the only member of the GPX family that can reduce hydroperoxy-phospholipids to nontoxic hydroxy-phospholipids utilizing glutathione (GSH) as the reducing equivalent (12). Insufficiency of GPX4 or GSH results in ferroptosis due to the accumulation of oxidized PE (PEox).

Dysregulation of key components of ferroptotic machinery including GSH depletion and lipid oxidation have been observed after experimental (13) and clinical (14) TBI. We therefore reasoned that PE peroxidation and ferroptotic death may be an important pathogenic pathway in TBI. We first characterized the neuroprotective effects of ferroptosis inhibition following pharmacologic induction of ferroptosis and *in vitro* TBI. Using a liquid chromatography tandem-mass spectrometry (LC-MS/MS)-based redox lipidomics approach, we investigated ferroptotic PEox death signals in the pericontusional cortex after controlled cortical impact (CCI) in mice. We further examined the role of ferroptosis through quantification of key ferroptotic enzymes and GSH in the ipsilateral cortex. Finally, we tested the ability of baicalein, a 12/15-LOX inhibitor, to attenuate ferroptotic signaling after CCI.

Materials and Methods

Materials

A GPX4 specific inhibitor, RAS-selective lethal compound 3 (RSL3), was purchased from Selleck Chemicals (Houston, TX). Unless otherwise indicated, reagents were purchased from Sigma-Aldrich (Saint Louis, MO).

In vitro TBI model

HT22 cells were a generous gift from Dr. David Schubert (The Salk Institute, La Jolla, CA). These cells were previously shown to undergo ferroptosis following RSL3 treatment (10). Cells were cultured in Dulbecco's modified Eagle's medium with 10% fetal bovine serum and 1% penicillin-streptomycin (37°C, 5% CO_2). *In vitro* TBI was performed using a well-established model of mechanical stretch injury (15). At 24 h prior to stretch, cells were trypsinized and seeded (400,000 cells/well) on silicone membranes within custom-made stainless-steel wells. Wells were fitted into the stretch apparatus, and a severe stretch injury (strain rate 10 s^{-1}, membrane deformation 50%, peak pressure 3–4 psi) was applied to simulate a similar strain field to that of our *in vivo* TBI model. Data from at least three independent experiments are presented in the Figures.

Cell death assessment

Cell death was assessed by measuring activity of lactate dehydrogenase released into the cell culture media using the Cytotoxicity Detection Kit as per manufacturer's instructions (Promega, Madison, WI).

In vivo TBI model

Experiments were approved by the Institutional Animal Care and Use Committee at the University of Pittsburgh. Care and handling of the animals were in accord with National Institutes of Health Guidelines. Adult male C57BL/6 mice (Jackson Laboratories, Bar Harbor, ME) were subjected to severe TBI as previously described (16). Anesthesia was induced with 3% isoflurane in N_2O:O_2 (70:30) and maintained with 1.5% isoflurane via nose cone, and rectal temperature was maintained at 37 ± 0.5°C. Animals were placed onto a stereotaxic frame and secured with ear bars. The bone overlying the left parietal cortex was removed. CCI was produced using a flat 3-mm pneumatically-driven impactor tip (6.0 ± 0.2

m/s, 50 ms dwell time, 1.4 mm depth). The bone flap was replaced and sealed, and the scalp incision was closed. Mice were monitored with supplemental O_2 (100%) for 1 h before returning to their cages. Baicalein (50 mg/kg) was administered via intraperitoneal injection (17–19) at 10–15 min post-CCI. Baicalein was dissolved in Cremophor El and ethanol (CEE) solution and diluted with normal saline (NS) (CEE:NS, 1:3, v/v). Separate experiments were performed for biochemical, histological and functional outcome testing with sample sizes of 4–6/group for the first two outcomes and 9–13 for the functional outcome. The number of animals used in each experiment is shown in Figure legends.

Lipid extraction and MS analysis

Lipid extraction of the pericontusional cortex was achieved using the Folch method. Total phosphate content of the lipid extracts was quantified using a micro-method (20). Extracted lipids (~30 nmol of total phospholipids) were added to a glass tube with 7.5 pmol of each deuterated internal standard (Table S1) and dried under N_2 flow. The dried film was dissolved in 15 μl of solvent A (hexane:2-propanol:water, 430:570:10, v/v/v), and 5 μl of the reconstituted sample was injected in duplicate into the LC-MS/MS system for phospholipid analysis. LC/MS analysis was performed using a Dionex UltiMate 3000 RSLCnano System coupled online to an Orbitrap Fusion™ Lumos™ Tribrid™ Mass Spectrometer (Thermo Fisher Scientific, San Jose, CA) using a normal-phase Silica (2) column (Luna 3 μm, 100 Å, 150 × 2.1 mm) (Phenomenex, Torrance, CA) as previously described (10). The MS data were analyzed using Compound Discoverer software (Thermo Fischer Scientific, San Jose, CA) as previously described (10).

Protein and GSH measurements

Ipsilateral cortex was sonicated in lysis buffer (Tris base 30 mM, NaCl 150 mM, Triton-X 0.5%, pH 7.4) with protease and phosphatase inhibitors (ThermoScientific-PIERCE, Rockford, IL). Samples were centrifuged (10 min, 16,000 g, 4°C), and supernatants were collected for protein and GSH measurements. Western blotting was performed using the following antibodies: GPX4 (1:500, ab125066), 15-LOX2 (1:200–500, sc-67143), ACSL4 (1:500, sc-13450), actin (1:1000, A3854), and horseradish peroxidase-conjugated antibodies (1:2000, ab97023/ab97051/ab6721). Bands were detected using Pierce ECL Western Blotting Substrate (ThermoFisher Scientific, San Jose, CA) and the ChemiDoc XRS+ System (Bio-Rad, Hercules, CA). NIH ImageJ software was utilized for densitometry analyses. GSH was measured using a fluorescent assay with ThioGlo-1 (Covalent Associates, Inc., Woburn, MA) as previously described (13).

Terminal deoxynucleotidyl transferase dUTP Nick-End Labeling (TUNEL) staining

Mice were perfused with heparinized saline followed by 4% paraformaldehyde. Brains were extracted, post-fixed (24 h, 4% paraformaldehyde), and embedded in paraffin. Using a Leitz 1512 Microtome (Leica Biosystems Inc., Buffalo Grove, IL), multiple 5-μm coronal sections of the dorsal hippocampus (200-μm intervals) were collected. The ApopTag Peroxidase In Situ Apoptosis Detection Kit (S7110) was used to detect TUNEL positivity according to the manufacturer's instruction (EMD Millipore, Billerica, MA). Briefly, tissue sections were deparaffinized and incubated with TdT enzyme and a mixture of digoxigenin-labeled and unlabeled nucleotides. Samples were subsequently incubated with fluorescein-conjugated

anti-digoxigenin antibody and counterstained with DAPI. Two consecutive, coronal sections of the dorsal hippocampus underlying the cortical contusion were stained, imaged, quantified, and averaged per animal. TUNEL-stained neurons were counted in the entire anatomic CA1, CA2, CA3, and dentate gyrus regions and normalized to area. TUNEL positivity was quantified per mm^2 in CA1, CA2, CA3, and dentate gyrus sections stained with TUNEL and DAPI (EMD Millipore, Billerica, MA). Images were obtained using a Nikon Eclipse E600 microscope, and analysis was performed using NIS Elements software (Nikon, Melville, NY).

Morris water maze (MWM) performance

The MWM task was used to assess acquisition of spatial learning (21). The maze consisted of a plastic pool (83 cm diameter, 60 cm height) filled with water (26 ± 1°C) to a depth of 29 cm and placed in a room with salient visual cues that remained unchanged. A clear Plexiglass platform (10 cm diameter, 28 cm height) was positioned 15 cm from the wall of the pool in the southwest quadrant for all trials. Acquisition of spatial learning was evaluated through four daily trials on POD 10–14, based on a lack of motor deficits in open field test between sham and CCI groups by POD 5 (Fig. S2). Trials lasted until the mouse reached the hidden platform or until 120 s had elapsed. Mice that failed to find the platform were manually guided to it, and all animals were kept on the platform for 10 s after each trial. Mice were placed in a heated incubator for 5 min between trials. On POD 15, the platform was made visible (2 cm above the water), and the task was repeated to assess deficits in visual and motor function. The ANY-Maze video tracking system (San Diego Instruments, San Diego, CA) was used to record MWM parameters.

Statistical Analysis

Statistical analyses of biochemical and histological data were performed using GraphPad Prism software (GraphPad Software, Inc., La Jolla, CA). Data were analyzed using Student's *t*-test or ANOVA with Tukey's post-hoc analysis for two- or multi-group comparisons, respectively. TFor the time to hidden platform endpoint in MWM task was analyzed with SAS 9.4 (SAS Institute Inc. Cary, NC) software. D, data were summarized as mean ± standard deviation (SD) for each group (i.e., sham, vehicle-CCI, or baicalein-CCI) on each day. PROC TRANSREG in SAS SAS 9.4 (SAS Institute Inc. Cary, NC) software was usedrun to check if a Box-Cox transformation (22) was necessary to make the data normally distributed. It was found that the data could be regarded as normally distributed after log-transformation. To test if the three groups had the same rate of decrease over the 5 days, a linear mixed model was built on the log-transformed data, where group and day and their interaction were used as fixed effects, and animal id was used as a random effect. For time to platform under visible condition, data were summarized as mean ± SD for each group. The comparison between groups was performed by one-way ANOVA followed by Tukey's multiple comparisons on log-transformed data. Statistical significance was set at $p<0.05$, and data are expressed as mean ± standard deviation.

Results

Ferroptosis inhibition rescues HT22 neurons from *in vitro* TBI

We first evaluated whether anti-ferroptotic agents could rescue neurons from death induced by pro-ferroptotic conditions (GSH or GPX4 insufficiency) or *in vitro* TBI. HT22 cells were exposed to RSL3 (inhibitor of GPX4) resulting in increased cell death that was rescued by inhibitors of key ferroptotic regulatory steps: ferrostatin-1 (Fer-1) (lipid radical-trapping antioxidant), triacsin C (ACSL4 inhibitor), and baicalein (12/15-LOX inhibitor) (Fig S1, 1A). Similar results were obtained with glutamate or erastin (inhibitors of cystine/glutamate antiporter which result in depletion of intracellular cysteine – the rate-limiting substrate of GSH synthesis) and L-buthionine sulfoximine (BSO; inhibitor of rate-limiting enzyme in GSH synthesis) (Fig. S1, S3A-C). Similarly, *in vitro* TBI elicited by mechanical stretch resulted in increased cell death that was significantly reduced with administration of Fer-1, triacsin C, baicalein, or liproxstatin-1 (Lip-1; lipid radical-trapping antioxidant) (Fig. 1B).

PE in mouse cortex contains more AA/AdA than other phospholipid classes

We previously showed that oxidation of AA/AdA-PE is a key step in ferroptosis execution (9). Therefore we next examined the cortical phospholipidome of uninjured mice using high-resolution LC-MS/MS. Among the identified phospholipid classes (Fig. S4A), abundance of AA/AdA-PE was higher than all other classes of AA/AdA-containing phospholipids (Fig. S4B), demonstrating an abundance of precursor for ferroptosis execution in the brain. The identity of AA/AdA-PE species was confirmed through MS^2 fragmentation (Fig. S5).

CCI results in phospholipid, protein, and GSH changes consistent with ferroptosis activation

As we had observed an abundance of AA/AdA-PE in mouse cortex, we next examined PE oxidation in naive and CCI-injured animals at 4 h after impact. LC-MS/MS analysis showed a significant increase in total PE oxidation (Fig. 2A) and individual oxidized-PE species (Fig. 2B) in pericontusional vs naive cortex. Identities of the significantly elevated PEox species (Fig. S6), confirmed with fragmentation analyses (Fig. S7), were consistent with ferroptotic mediators previously identified by our group (9). Fragmentation analyses of PEox demonstrated a predominance of 15-LOX products including 15-hydroperoxyeicosatetraenoic acid.

In line with the predominance of 15-LOX-generated oxidized lipid products, 15-LOX2 expression was significantly elevated post-CCI vs naive (Fig. 3A,B). ACSL4 was also significantly elevated after injury (Fig. 3A,B). Expression of GPX4 remained unchanged (Fig. 3A,B), and GSH levels were significantly decreased after injury (Fig. 3C). Overall, the protein and GSH profile in injured brain reflected a shift toward a pro-oxidative lipid environment (15-LOX2 and ACSL4) without a compensatory increase in lipid-hydroperoxide reducing capacity (GPX4 and GSH).

LOX inhibition results in histological neuroprotection and decreased PE oxidation after CCI

With strong evidence for a role of 15-LOX in the pathogenesis of CCI, we sought to determine whether LOX inhibition via baicalein affected neuronal death and ferroptotic PE oxidation. Baicalein-treated animals demonstrated significantly less hippocampal TUNEL positivity than vehicle-treated mice post-CCI (Fig. 4A-C). Because both ferroptotic (23) and apoptotic cells can be detected with TUNEL, we assessed cardiolipin (CL) oxidation. Oxidation of CL through cytochrome C/CL complex by H_2O_2 is known to result in the release of pro-apoptotic signals (24). Non-oxidized CL decreased, and oxidized CL increased in the cortex after CCI. However, these changes in CL oxidation were not affected by baicalein administration (Fig. S8). Conversely baicalein significantly attenuated PE oxidation, particularly pro-ferroptotic PE(38:5)+3O and PE(40:5)+3O species (9, 10) after CCI vs vehicle (Fig. 2A,B, S6).

LOX inhibition results in functional improvement after CCI

We next evaluated the effect of baicalein on functional outcome after CCI using the MWM task. Based on the linear mixed model on log(time to platform), the interaction of group and day was not significant (p=0.5797) thus, we removed the interaction term from the model and re-fit the data. We found that the relationship of time to platform with group and day was in the following, where numbers in the parentheses are the corresponding standard errors:

$$\begin{aligned}
&\text{Sham:} && \log(\text{time to platform}) = 3.72(0.13) - 0.22(0.03)^{*}\,\text{day}\\
&\text{Vehicle} - \text{CCI:} && \log(\text{time to platform}) = 4.31(0.12) - 0.22(0.03)^{*}\,\text{day}\\
&\text{Baicalein} - \text{CCI:} && \log(\text{time to platform}) = 3.91(0.12) - 0.22(0.03)^{*}\,\text{day}
\end{aligned}$$

To test for the average difference between the three groups, we ran F-tests in this model and obtained the results summarized in Table 1. Overall, the three groups did not have significant difference in slope of change, and over the 5 days the vehicle-CCI group had significantly longer time to platform than the sham and the baicalein-CCI groups, but there was no difference between sham and baicalein-CCI (Table 1, Fig. 4D). Under visible platform conditions, the three groups did not have significant difference (Table S2) indicating a lack of motor of visual deficit. A one-way ANOVA for time spent in the target quadrant during probe trial revealed a significant group main effect (p=0.0009). Post-hoc analysis showed that CCI-injured groups spent significantly less time in the target quadrant than shams, but the baicalein-CCI group was not different than the vehicle-CCI group (Fig. S9).

Discussion

Since the recent identification of ferroptosis as a distinct cell death pathway, its role in disease pathogenesis is increasingly recognized (10, 25–28). Several lines of evidence suggest that ferroptosis may be particularly important in the brain: 1) Brain contains the highest PUFA content in the body, and thus possesses abundant precursor for lipid peroxidation (29). 2) GSH depletion and lipid peroxidation are associated with neurodegenerative disease including TBI (30). 3) Genetic deficiency of GPX4 results in

neuronal death *in vitro* and *in vivo* (31–34). Here we provide evidence that ferroptosis contributes to neuronal death and functional outcome after TBI. To our knowledge, this study is the first study directly examining ferroptosis inhibition in both *in vitro* and *in vivo* TBI.

Several studies have evaluated ferroptosis in models of acute brain injury. The earliest study utilized a rat organotypic hippocampal slice culture model to examine ferroptosis after glutamate excitotoxicity (7) – a key phenomenon in neurodegeneration and brain trauma (35). Co-incubation with Fer-1 or ciclopirox (iron chelator) significantly attenuated glutamate-induced cell death (7). Neuroprotective effects of ferroptosis inhibition were recently shown in intracerebral hemorrhage models (36, 37). Interestingly, lipid oxidation was reported to have a detrimental effect on the transition of astrocytes and fibroblasts into neurons after TBI (38). Treatment with Lip-1 enhanced *in vitro* astrocyte conversion efficiency, while α-tocotrienol enhanced conversion efficiency in a penetrating brain injury model. Finally, we recently reported that 15-LOX expression and activity were increased and GPX4 expression and activity were decreased with co-localization of 15-LOX and PEBP1 in the hippocampus after CCI in a developmental TBI model in post-natal day 17 rats. Furthermore we showed that ferroptotic PEox species were increased in the cortex (10). Together these data indicated that biomarkers of ferroptosis increase after CCI in the immature brain. In addition that study established that formation of the complex of 15-LOX and PEBP1 changed the substrate specificity of 15-LOX from free arachidonic acid to arachidonic acid esterified into PE. The current study extends these observations to adult mice and shows that baicalein post-treatment decreased ferroptotic PEox after CCI. In addition, we show that ferroptosis inhibitors, including baicalein, attenuate mechanical stretch- induced death in HT22 hippocampal neuronal cells suggesting that this *in vitro* TBI model might be useful for therapeutic screening of drugs targeting ferroptosis. Furthemore, future studies evaluating the quantitative contribution of this pathway compared to other apoptotic and necrotic death pathways could be revealing (15, 39, 40).

Though several studies have shown neuroprotective effects of Fer-1 *in vivo*, Fer-1 has limited biological availability (41), and it is possible that targeting upstream in this pathway at the level of lipid peroxidation may be more effective. While cyclooxygenases and cytochrome P450 can catalyze lipid oxidation (42), to date only a role of the LOX family has been demonstrated in ferroptosis (32, 43, 44). In humans, the LOX family is comprised of 6 functional isoforms which differ in their preferred carbon for oxidation with respect to AA (45). Species and tissue variation of LOX isoforms (45) and lack of structural information for human LOX isoforms (27) make pharmacologic inh1ibition of LOX as an anti-ferroptotic strategy challenging. Furthermore, specific disruptors of 15LOX-PEBP1 complexes might be more effective as anti-ferroptotic compounds. Isoform-specific LOX inhibitors are under development (46) and may inhibit ferroptosis more efficiently than non-specific or pan-LOX inhibitors.

As 15-LOX2-specific inhibitors are currently unavailable, we assessed the effects of baicalein in our TBI model. Baicalein is a polyphenolic flavonoid and 12/15-LOX inhibitor (47). Compared to synthetic, anti-ferroptotic agents such as Lip-1 and Fer-1, baicalein is an herbal supplement found in natural products, which may more rapidly facilitate its use in

clinical settings. The importance of 12/15-LOX and the protective effects of baicalein are well-studied in models of focal cerebral ischemia (48, 49). While one study has demonstrated improved motor function and decreased number of FluoroJade B-positive neurons with baicalein treatment immediately post-CCI in rats, this study focused on an anti-inflammatory mechanism to explain its protective effects (19).

To our knowledge, our study represents the first analysis of baicalein administration for ferroptosis inhibition after TBI. The versatile chemical structure of Baicalein makes it a non-narrowly specific LOX inhibitor with several alternative mechanisms of action (19, 50). However, given that 15-LOX is responsible for the production of pro-ferroptotic PEox species (9–11) and our redox lipidomics data demonstrate that baicalein attenuated accumulation of these PEox after CCI, without affecting pro-apoptotic cardiolipin oxidation, we suggest that baicalein's effects are due, at least in part, to its inhibitory effects on 15-LOX. Currently hydroperoxy-arachidonoyl- and adrenoyl-PE species are the most reliable quantitative predictive markers of ferroptosis (51). While we observed functional and histological protection with early (10–15 min) baicalein administration post-CCI, delayed drug delivery may be more practical in clinical settings.

While we observed effects of baicalein on proferroptotic PEox generation, hippocampal cell death, and spatial memory acquisition in MWM task, baicalein did not affect memory retention assessed by the probe trial or lesion volume in our study. This could be due to multiple mechanisms of action of baicalein as well as suboptimal drug dosing or timing(19, 50). Bilateral hippocampal lesions are required to produce significant MWM deficits in rodents in the absence of trauma(52). However numerous studies have shown that unilateral CCI leads to neuronal death in the hippocampus (primarily in the CA3 region) and results in MWM deficits(53, 54). Furthermore previous studies have shown improvement in MWM performance without an effect on lesion volume after CCI with treatment(55, 56). This is in line with the data showing that MWM has important non-hippocampal components(57). Indeed even the mice that have bilateral intrahippocampal excitotoxic lesions can significantly improve in acquisition of spatial memory during training(57). In recent years, the role of entorhinal cortex in spatial learning and memory has been elucidated. Medial entorhinal cortex, especially in layer 2, has been identified as having place cells and communicating with place cells in the hippocampus(58, 59). Entorhinal cortex is one of the affected regions after CCI in mice(54). Our redox lipidomics analysis of the pericontusional cortex showed that baicalein attenuated CCI-induced proferroptotic PEox species. In addition to hippocampus and entorhinal cortex, white matter injury can also affect MWM outcome after CCI in mice(60). White matter lesions may affect procedural learning component of MWM(61, 62).

Conclusions

In conclusion, ferroptosis inhibition may represent a viable therapeutic target for neuroprotection following TBI. Here we demonstrated changes in PE oxidation, protein expression, and GSH levels that were consistent with ferroptosis activation post-CCI. Baicalein administration significantly reduced cell death following ferroptosis induction, *in*

vitro TBI, and *in vivo* TBI. Furthermore, baicalein attenuated PE oxidation and provided histological and cognitive protection post-injury.

Supplementary Material

Refer to Web version on PubMed Central for supplementary material.

Acknowledgements

We thank Henry Alexander for technical assistance with CCI experiments. The work is supported, in part, by NIH grants (NS061817, NS076511, AI068021, NS079061).

References

1. Prevention CfDCa. Report to Congress on Traumatic Brain Injury in the United States: Epidemiology and Rehabilitation In: Prevention. NCfIPaCDoUI, editor. Atlanta, GA; 2015.
2. Thurman DJ, Alverson C, Dunn KA, et al. Traumatic brain injury in the United States: A public health perspective. The Journal of head trauma rehabilitation 1999;14(6):602–615. [PubMed: 10671706]
3. Selassie AW, Zaloshnja E, Langlois JA, et al. Incidence of long-term disability following traumatic brain injury hospitalization, United States, 2003. The Journal of head trauma rehabilitation 2008;23(2):123–131. [PubMed: 18362766]
4. Finkelstein E, Corso PS, Miller TR. The incidence and economic burden of injuries in the United States: Oxford University Press, USA; 2006.
5. Coronado VG, McGuire LC, Faul M, et al. Traumatic brain injury epidemiology and public health issues. Brain injury medicine: Principles and practice 2012;84.
6. Roozenbeek B, Maas AI, Menon DK. Changing patterns in the epidemiology of traumatic brain injury. Nature reviews Neurology 2013;9(4):231–236. [PubMed: 23443846]
7. Dixon SJ, Lemberg KM, Lamprecht MR, et al. Ferroptosis: An Iron-Dependent Form of Non-Apoptotic Cell Death. Cell 2012;149(5):1060–1072. [PubMed: 22632970]
8. Stockwell BR, Friedmann Angeli JP, Bayir H, et al. Ferroptosis: A Regulated Cell Death Nexus Linking Metabolism, Redox Biology, and Disease. Cell;171(2):273–285. [PubMed: 28985560]
9. Kagan VE, Mao G, Qu F, et al. Oxidized arachidonic and adrenic PEs navigate cells to ferroptosis. Nature chemical biology 2017;13(1):81–90. [PubMed: 27842066]
10. Wenzel SE, Tyurina YY, Zhao J, et al. PEBP1 Wardens Ferroptosis by Enabling Lipoxygenase Generation of Lipid Death Signals. Cell;171(3):628–641.e626. [PubMed: 29053969]
11. Doll S, Proneth B, Tyurina YY, et al. ACSL4 dictates ferroptosis sensitivity by shaping cellular lipid composition. Nature chemical biology 2017;13(1):91–98. [PubMed: 27842070]
12. Angeli JPF, Schneider M, Proneth B, et al. Inactivation of the ferroptosis regulator Gpx4 triggers acute renal failure in mice. Nature cell biology 2014;16(12):1180–1191. [PubMed: 25402683]
13. Tyurin VA, Tyurina YY, Borisenko GG, et al. Oxidative stress following traumatic brain injury in rats: quantitation of biomarkers and detection of free radical intermediates. Journal of neurochemistry 2000;75(5):2178–2189. [PubMed: 11032908]
14. Bayir H, Kagan VE, Tyurina YY, et al. Assessment of antioxidant reserves and oxidative stress in cerebrospinal fluid after severe traumatic brain injury in infants and children. Pediatric research 2002;51(5):571–578. [PubMed: 11978879]
15. Ji J, Kline AE, Amoscato A, et al. Lipidomics identifies cardiolipin oxidation as a mitochondrial target for redox therapy of brain injury. Nature neuroscience 2012;15(10):1407–1413. [PubMed: 22922784]
16. Whalen MJ, Clark RS, Dixon CE, et al. Reduction of cognitive and motor deficits after traumatic brain injury in mice deficient in poly(ADP-ribose) polymerase. Journal of cerebral blood flow and metabolism : official journal of the International Society of Cerebral Blood Flow and Metabolism 1999;19(8):835–842.

17. Im HI, Joo WS, Nam E, et al. Baicalein prevents 6-hydroxydopamine-induced dopaminergic dysfunction and lipid peroxidation in mice. Journal of pharmacological sciences 2005;98(2):185–189. [PubMed: 15942123]
18. Wei N, Wei Y, Li B, et al. Baicalein Promotes Neuronal and Behavioral Recovery After Intracerebral Hemorrhage Via Suppressing Apoptosis, Oxidative Stress and Neuroinflammation. Neurochemical research 2017;42(5):1345–1353. [PubMed: 28108850]
19. Chen SF, Hsu CW, Huang WH, et al. Post-injury baicalein improves histological and functional outcomes and reduces inflammatory cytokines after experimental traumatic brain injury. British journal of pharmacology 2008;155(8):1279–1296. [PubMed: 18776918]
20. Böttcher C, Pries C. A rapid and sensitive sub-micro phosphorus determination. Analytica Chimica Acta 1961;24:203–204.
21. Hamm RJ, Dixon CE, Gbadebo DM, et al. Cognitive deficits following traumatic brain injury produced by controlled cortical impact. Journal of neurotrauma 1992;9(1):11–20. [PubMed: 1619672]
22. Box GE, Cox DR. An analysis of transformations. Journal of the Royal Statistical Society Series B (Methodological) 1964:211–252.
23. Friedmann Angeli JP, Schneider M, Proneth B, et al. Inactivation of the ferroptosis regulator Gpx4 triggers acute renal failure in mice. Nat Cell Biol 2014;16(12):1180–1191. [PubMed: 25402683]
24. Kagan VE, Tyurin VA, Jiang J, et al. Cytochrome c acts as a cardiolipin oxygenase required for release of proapoptotic factors. Nat Chem Biol 2005;1(4):223–232. [PubMed: 16408039]
25. Cao JY, Dixon SJ. Mechanisms of ferroptosis. Cell Mol Life Sci 2016;73(11–12):2195–2209. [PubMed: 27048822]
26. Yang WS, Stockwell BR. Ferroptosis: Death by Lipid Peroxidation. Trends Cell Biol 2016;26(3): 165–176. [PubMed: 26653790]
27. Angeli JPF, Shah R, Pratt DA, et al. Ferroptosis Inhibition: Mechanisms and Opportunities. Trends Pharmacol Sci 2017;38(5):489–498. [PubMed: 28363764]
28. Tonnus W, Linkermann A. The in vivo evidence for regulated necrosis. Immunol Rev 2017;277(1): 128–149. [PubMed: 28462528]
29. Bazinet RP, Laye S. Polyunsaturated fatty acids and their metabolites in brain function and disease. Nat Rev Neurosci 2014;15(12):771–785. [PubMed: 25387473]
30. Bayir H, Kochanek PM, Kagan VE. Oxidative stress in immature brain after traumatic brain injury. Developmental neuroscience 2006;28(4–5):420–431. [PubMed: 16943665]
31. Yoo SE, Chen L, Na R, et al. Gpx4 ablation in adult mice results in a lethal phenotype accompanied by neuronal loss in brain. Free radical biology & medicine 2012;52(9):1820–1827. [PubMed: 22401858]
32. Seiler A, Schneider M, Forster H, et al. Glutathione peroxidase 4 senses and translates oxidative stress into 12/15-lipoxygenase dependent- and AIF-mediated cell death. Cell metabolism 2008;8(3):237–248. [PubMed: 18762024]
33. Hambright WS, Fonseca RS, Chen L, et al. Ablation of ferroptosis regulator glutathione peroxidase 4 in forebrain neurons promotes cognitive impairment and neurodegeneration. Redox Biology 2017;12:8–17. [PubMed: 28212525]
34. Chen L, Hambright WS, Na R, et al. Ablation of the Ferroptosis Inhibitor Glutathione Peroxidase 4 in Neurons Results in Rapid Motor Neuron Degeneration and Paralysis. The Journal of biological chemistry 2015;290(47):28097–28106. [PubMed: 26400084]
35. Platt SR. The role of glutamate in central nervous system health and disease–a review. The Veterinary Journal 2007;173(2):278–286. [PubMed: 16376594]
36. Li Q, Han X, Lan X, et al. Inhibition of neuronal ferroptosis protects hemorrhagic brain. JCI insight 2017;2(7).
37. Zille M, Karuppagounder SS, Chen Y, et al. Neuronal Death After Hemorrhagic Stroke In Vitro and In Vivo Shares Features of Ferroptosis and Necroptosis. Stroke 2017;48(4):1033–1043. [PubMed: 28250197]
38. Gascon S, Murenu E, Masserdotti G, et al. Identification and Successful Negotiation of a Metabolic Checkpoint in Direct Neuronal Reprogramming. Cell stem cell 2016;18(3):396–409. [PubMed: 26748418]

39. You Z, Savitz SI, Yang J, et al. Necrostatin-1 Reduces Histopathology and Improves Functional Outcome After Controlled Cortical Impact In Mice. Journal of cerebral blood flow and metabolism : official journal of the International Society of Cerebral Blood Flow and Metabolism 2008;28(9):1564–1573.
40. Clark RSB, Bayir H, Chu CT, et al. Autophagy is increased in mice after traumatic brain injury and is detectable in human brain after trauma and critical illness. Autophagy 2008;4(1):88–90. [PubMed: 17957135]
41. Linkermann A, Skouta R, Himmerkus N, et al. Synchronized renal tubular cell death involves ferroptosis. Proceedings of the National Academy of Sciences of the United States of America 2014;111(47):16836–16841. [PubMed: 25385600]
42. Anthonymuthu TS, Kenny EM, Bayir H. Therapies targeting lipid peroxidation in traumatic brain injury. Brain research 2016;1640(Pt A):57–76. [PubMed: 26872597]
43. Li Y, Maher P, Schubert D. A role for 12-lipoxygenase in nerve cell death caused by glutathione depletion. Neuron 1997;19(2):453–463. [PubMed: 9292733]
44. Yang WS, Kim KJ, Gaschler MM, et al. Peroxidation of polyunsaturated fatty acids by lipoxygenases drives ferroptosis. Proceedings of the National Academy of Sciences of the United States of America 2016;113(34):E4966–4975. [PubMed: 27506793]
45. Kuhn H, Banthiya S, van Leyen K. Mammalian lipoxygenases and their biological relevance. Biochimica et biophysica acta 2015;1851(4):308–330. [PubMed: 25316652]
46. Jameson JB, 2nd, Kantz A, Schultz L, et al. A high throughput screen identifies potent and selective inhibitors to human epithelial 15-lipoxygenase-2. PloS one 2014;9(8):e104094. [PubMed: 25111178]
47. Lapchak PA, Maher P, Schubert D, et al. Baicalein, an antioxidant 12/15-lipoxygenase inhibitor improves clinical rating scores following multiple infarct embolic strokes. Neuroscience 2007;150(3):585–591. [PubMed: 17942241]
48. van Leyen K, Kim HY, Lee SR, et al. Baicalein and 12/15-lipoxygenase in the ischemic brain. Stroke 2006;37(12):3014–3018. [PubMed: 17053180]
49. Jin G, Arai K, Murata Y, et al. Protecting against cerebrovascular injury: contributions of 12/15-lipoxygenase to edema formation after transient focal ischemia. Stroke 2008;39(9):2538–2543. [PubMed: 18635843]
50. Lin YL, Lin RJ, Shen KP, et al. Baicalein, isolated from Scutellaria baicalensis, protects against endothelin-1-induced pulmonary artery smooth muscle cell proliferation via inhibition of TRPC1 channel expression. Journal of ethnopharmacology 2011;138(2):373–381. [PubMed: 21963569]
51. Stockwell BR, Friedmann Angeli JP, Bayir H, et al. Ferroptosis: A Regulated Cell Death Nexus Linking Metabolism, Redox Biology, and Disease. Cell 2018;171(2):273–285.
52. Moser E, Moser MB, Andersen P. Spatial learning impairment parallels the magnitude of dorsal hippocampal lesions, but is hardly present following ventral lesions. The Journal of neuroscience : the official journal of the Society for Neuroscience 1993;13(9):3916–3925. [PubMed: 8366351]
53. Kline AE, Massucci JL, Marion DW, et al. Attenuation of working memory and spatial acquisition deficits after a delayed and chronic bromocriptine treatment regimen in rats subjected to traumatic brain injury by controlled cortical impact. Journal of neurotrauma 2002;19(4):415–425. [PubMed: 11990348]
54. Colicos MA, Dixon CE, Dash PK. Delayed, selective neuronal death following experimental cortical impact injury in rats: possible role in memory deficits. Brain research 1996;739(1–2):111–119. [PubMed: 8955931]
55. Khuman J, Zhang J, Park J, et al. Low-level laser light therapy improves cognitive deficits and inhibits microglial activation after controlled cortical impact in mice. Journal of neurotrauma 2012;29(2):408–417. [PubMed: 21851183]
56. Lok J, Wang H, Murata Y, et al. Effect of neuregulin-1 on histopathological and functional outcome after controlled cortical impact in mice. Journal of neurotrauma 2007;24(12):1817–1822. [PubMed: 18159993]
57. Gerlai RT, McNamara A, Williams S, et al. Hippocampal dysfunction and behavioral deficit in the water maze in mice: an unresolved issue? Brain research bulletin 2002;57(1):3–9. [PubMed: 11827731]

58. Hafting T, Fyhn M, Molden S, et al. Microstructure of a spatial map in the entorhinal cortex. Nature 2005;436(7052):801–806. [PubMed: 15965463]

59. Vorhees CV, Williams MT. Assessing spatial learning and memory in rodents. ILAR journal 2014;55(2):310–332. [PubMed: 25225309]

60. An C, Jiang X, Pu H, et al. Severity-Dependent Long-Term Spatial Learning-Memory Impairment in a Mouse Model of Traumatic Brain Injury. Translational stroke research 2016;7(6):512–520. [PubMed: 27539574]

61. Bannerman DM, Good MA, Butcher SP, et al. Distinct components of spatial learning revealed by prior training and NMDA receptor blockade. Nature 1995;378(6553):182–186. [PubMed: 7477320]

62. Gerlai R Behavioral tests of hippocampal function: simple paradigms complex problems. Behavioural brain research 2001;125(1–2):269–277. [PubMed: 11682118]

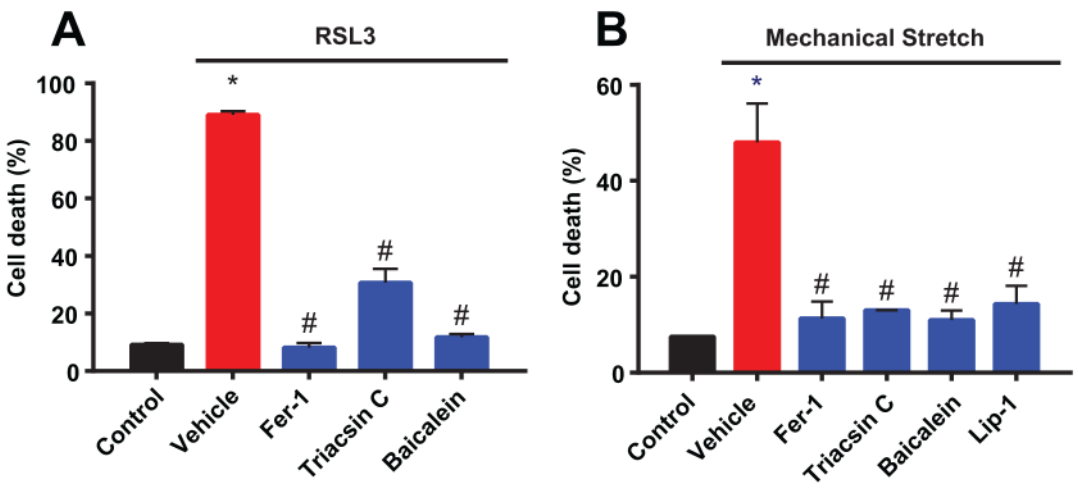

Figure 1. Inhibition of ferroptosis rescues HT22 neurons from pharmacologically-induced cell death and *in vitro* traumatic brain injury (TBI).

(**A**) Ferroptosis was induced using RSL3 (50 nM; inhibitor of GPX4) resulting in a significant increase in cell death (lactate dehydrogenase release). Administration of Fer-1 (0.2-1 μM; lipid radical-trapping antioxidant), triacsin C (9.6 μM; ACSL4 inhibitor), or baicalein (5 μM; 12/15-LOX inhibitor) resulted in a significant reduction in RSL3-induced cell death. (**B**) HT22 neurons were subjected to severe mechanical stretch injury (3-4 psi), resulting in a significant increase in cell death that was rescued with Fer-1 (0.4 μM), triacsin C (10 μM), baicalein (5 μM), or liproxstatin-1 (40 nM; lipid radical-trapping antioxidant) administration. (Data are Mean ± SD, N=3-4/group, *p<0.05 vs control, #p<0.05 vs vehicle). Abbreviations: arachidonic acid (AA), adrenic acid (AdA), hydroperoxyl-phosphatidylethanolamine (PE-OOH), hydroxy-phosphatidylethanolamine (PE-OH), acyl-CoA synthetase long-chain family member 4 (ACSL4), lipoxygenase (LOX), glutathione peroxidase 4 (GPX4), glutathione (GSH), glutathione disulfide (GSSG), L-buthionine sulfoximine (BSO), RAS-selective lethal compound 3 (RSL3), deferoxamine (DFO), liproxstatin-1 (Lip-1), ferrostatin-1(Fer-1).

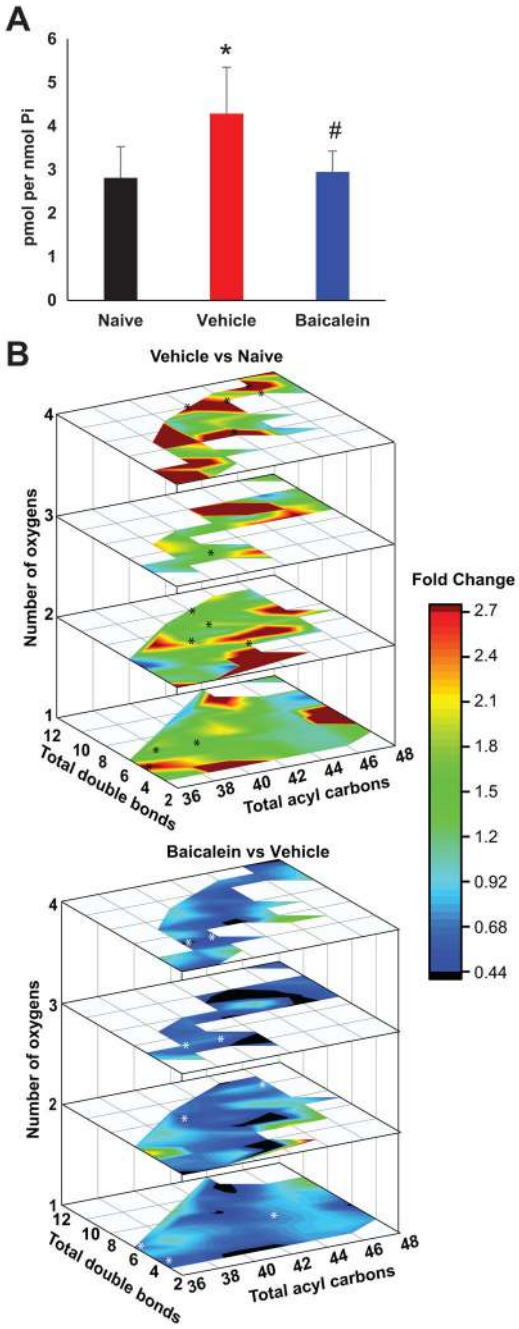

Figure 2. Baicalein administration reduces phosphatidylethanolamine (PE) oxidation in the cortex after controlled cortical impact (CCI).

(**A**) CCI resulted in a significant increase in total PE oxidation at 4 h after injury. The increase in PE oxidation was attenuated with baicalein administration. (**B**) Contour map demonstrating the speciation of PE oxidation in the cortex of vehicle-treated animals compared to naive (top) and baicalein-treated animals compared to vehicle-treated animals (bottom) at 4 h post-CCI. (Data are Mean ± SD, N=4-5/group, *p<0.05 vs naive, #p<0.05 vs vehicle).

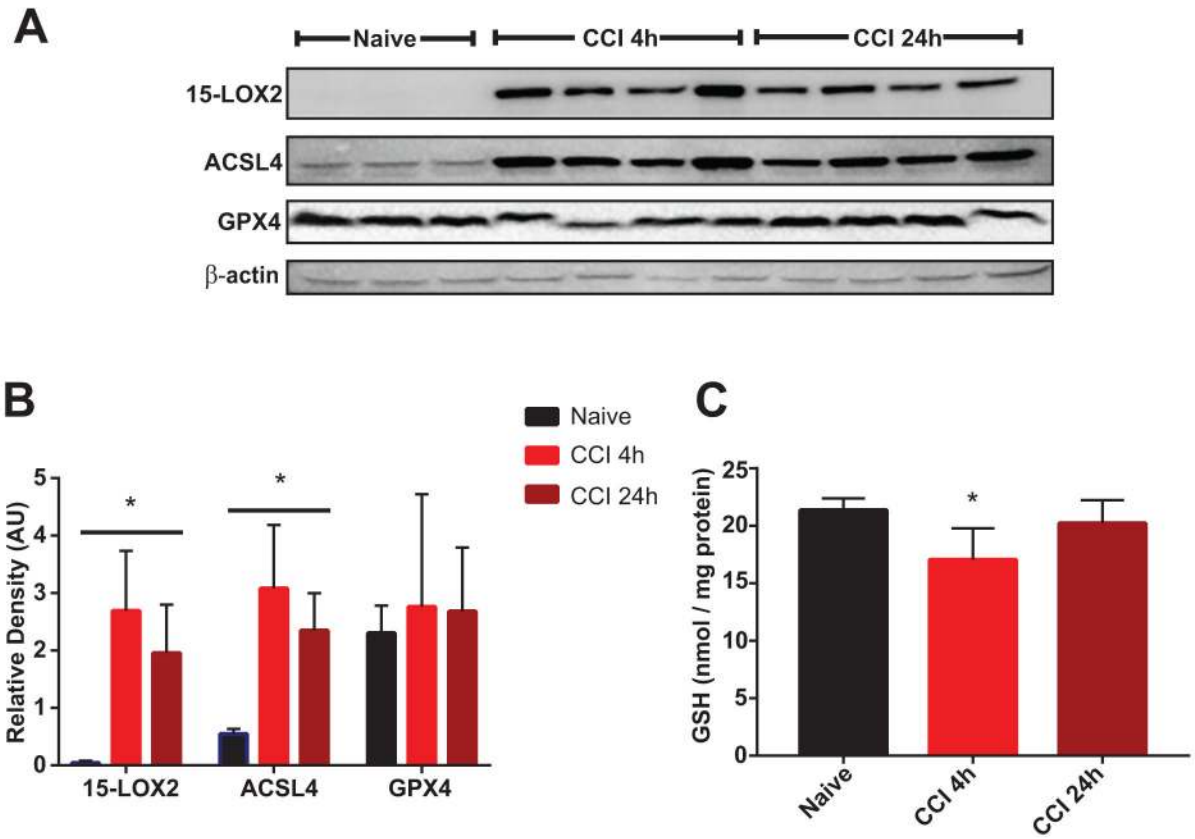

Figure 3. Controlled cortical impact (CCI) results in protein and glutathione (GSH) changes consistent with ferroptosis activation in the cortex.

Cortical expression of 15-lipoxygenase 2 (15-LOX2), acyl-CoA synthetase long-chain family member 4 (ACSL4), and glutathione peroxidase (GPX4) were measured in naive and CCI groups. (**A, B**) CCI resulted in a significant increase in 15-LOX2 (60-fold and 45-fold) and ACSL4 (6-fold and 4-fold) expression in cortex vs naive at 4 and 24 h after injury, respectively. GPX4 expression did not significantly differ between naive and CCI groups. (Data are Mean ± SD, N=3-4/group, *p<0.05 vs naive). (**C**) GSH was significantly depleted in cortex at 4 h post-CCI with respect to naive. (Data are Mean ± SD, N=4-5/group, *p<0.05 vs naive).

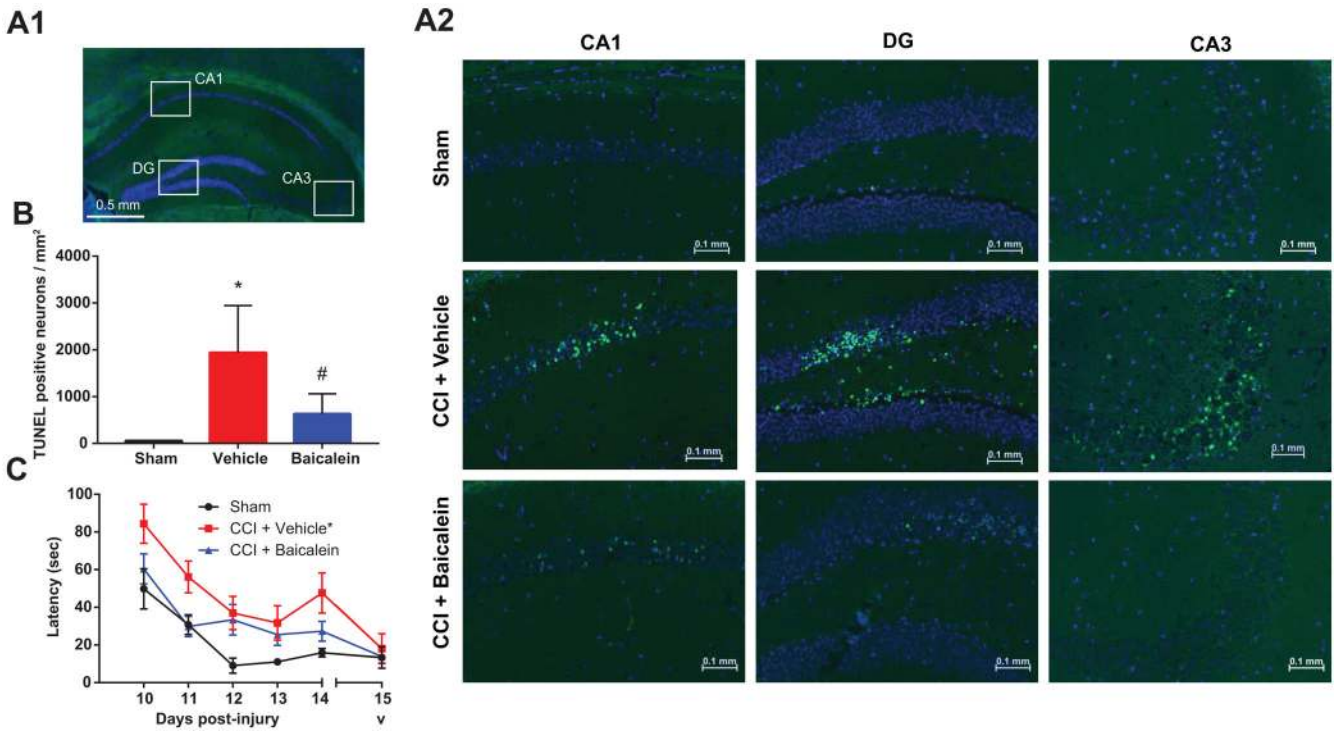

Figure 4. Baicalein administration results in decreased TUNEL positivity and improved Morris water maze (MWM) performance after controlled cortical impact (CCI).

(**A**) White boxes indicate areas of interest, shown in higher magnification in panel B. (**B**) Representative fluorescent images of DAPI and TUNEL staining in ipsilateral dentate gyrus (DG), CA1, and CA3 at 24 h after sham or CCI with baicalein or vehicle treatment. . (**C**) Quantitativape assessment of TUNEL-positive cells in the hippocampus showed a significant decrease in TUNEL positivity with baicalein compared to vehicle treatment following CCI. (Data are Mean ± SD, N=4-5/group, *p<0.05 vs sham, #p<0.05 vs vehicle). (**D**) Line graph showing the swim latency to reach the hidden platform on days 10-14 post-CCI and visible (v) platform on day 15 post-CCI in MWM testing. There was no significant difference in time to reach the visible platform between sham, CCI+vehicle, and CCI+baicalein groups, indicating a lack of motor of visual deficit. (Data are Mean ± SE, N=9-10/group, *p<0.05 vs. sham and baicalein-CCI).

Table 1.

Average difference between the three groups for time to hidden platform

Comparison	p-value for the comparison of average time to platform using F-test in the mixed model	Adjusted p value with the Holm multiple comparison adjustment procedure
Vehicle-CCI vs Sham	0.0010	0.0030
Baicalein-CCI vs Sham	0.2580	0.2580
Baicalein-CCI vs Vehicle-CCI	0.0145	0.0290